Bubble Column Reactors for Wastewater Treatment. 2. The Effect of Sparger Design on Sublation Column Hydrodynamics in the Homogeneous Flow Regime†

ARTICLE *in* INDUSTRIAL & ENGINEERING CHEMISTRY RESEARCH · MAY 1996

Impact Factor: 2.59 · DOI: 10.1021/ie950366y

4 AUTHORS, INCLUDING:

Kalliat Valsaraj
Louisiana State University
232 PUBLICATIONS **3,641** CITATIONS

Bubble Column Reactors for Wastewater Treatment. 2. The Effect of Sparger Design on Sublation Column Hydrodynamics in the Homogeneous Flow Regime†

Jeffrey S. Smith, Louis F. Burns, Kalliat T. Valsaraj,* and Louis J. Thibodeaux

Department of Chemical Engineering, Louisiana State University, Baton Rouge, Louisiana 70803

A simple analysis of bubble column hydrodynamics indicates that the upper limit of the homogeneous flow regime is the optimum operating condition for solvent sublation. This is in contrast to the traditional belief that solvent sublation is limited to the string bubbling flow regime. The implication is that the limited number of low-pressure adsorptive processes that operate in the bubbly flow regime, such as solvent sublation, may soon become viable options for industry. Results of gas holdup, bubble size, and dispersion experiments are reported as functions of gas velocity for three different types of gas-bubble spargers, namely, a fine porous glass frit, a flexible rubber membrane, and an annular shear sparger. The data show that the shear sparger affects the column dynamic properties such that the transition to the heterogeneous regime is delayed. Therefore, for applications requiring homogeneous flow, column capacity can be improved by approximately 25%. Moreover, the interfacial area produced by the shear sparger operating in the homogeneous regime rivals that produced by perforated and sintered plates operating in the heterogeneous regime.

Introduction

Hydrophobic organic compounds which possess very low aqueous solubilities and vapor pressures represent a significant portion of the pollutants found in the environment. These compounds are mostly neutral and nonpolar and are often found in very dilute concentrations in aqueous systems. One of the challenges that faces environmental engineers today is the cost-effective separation of these compounds from aqueous systems. Solvent sublation is a technology which has the potential to meet this challenge (Valsaraj, 1995). As described in part 1 of this series, solvent sublation is an adsorptive bubble process which exploits the surface-active nature of hydrophobic organic compounds to remove them from wastewaters. As air bubbles rise through a column of water, pollutant molecules adsorb upon the air−water interface. At the top of the column, the pollutant molecules are captured into an overlying organic solvent layer.

Historically, solvent sublation experiments have been conducted within the "string bubbling" flow regime (Ishii and Zuber, 1975; Geary, 1992). This flow regime is characterized by superficial gas velocities less than about 0.2 cm/s and bubble diameters less than 1 mm. Bubble coalescence is virtually nonexistent in this regime because the bubbles do not interact with one another as they rise up the column. The motivation for operating in this regime has been based on the fact that in solvent sublation, the *driving force* for mass transfer ($C_w - C_A/H$) is a function of the bubble size. It was shown in part 1 of this series that the effective Henry's law constant, H, is inversely related to the bubble radius. Since large values of H are desirable, the consensus of previous investigators has been that the fate of solvent sublation hinges on the ability to generate and maintain small bubbles (Valsaraj *et al.*, 1991).

Though small bubbles are desirable and are very important to sublation performance, the problem with placing too much emphasis on bubble size is that the effect of gas holdup on the overall interfacial area per unit volume is neglected. This has been the case in past sublation models (Valsaraj and Thibodeaux, 1991; Shibata and Tokunaga, 1994) which have been derived from the analysis of one bubble rather than the total gas volume contacting the water. Since all of the experimental data to date have been collected at very low gas velocity (low gas holdup), these models have worked well; however, they do not apply outside the string bubbling flow regime and cannot be used for extrapolation. Consequently, the general belief that scaleup is limited is not accurate.

In part 1 of this series, we presented a model for solvent sublation which included the effects of gas holdup and suggested that the bubbly flow or homogeneous regime is the appropriate operating regime. In this paper, we use well-accepted correlations and observations cited from bubble column hydrodynamic studies to show that this is indeed the case. We then discuss how small improvements in gas sparger design can delay the transition to the heterogeneous regime, thus improving the capacity of solvent sublation. Finally, we present hydrodynamic data collected from pilot sublation columns equipped with a variety of gas spargers (described under Apparatus) and briefly discuss how the data affect the interfacial area.

(a) Flow Regime for Solvent Sublation. Bubble column processes are often classified by the flow regime in which they operate (Geary, 1992). Figure 1 illustrates the different types of two-phase flow that are observed. As already alluded to, each flow regime is usually defined in terms of superficial gas velocity. For instance, the string bubbling flow regime occurs at < 0.2 cm/s. At higher velocities, $0.2 < u_g < \sim 4$ cm/s (homogeneous regime), the number of bubbles and their size increase, as shown in the figure. In this regime, the bubbles making up the swarm still behave somewhat independently. The bubbles are of uniform size, varying from 2 to 6 mm; gas holdup is radially uniform; and liquid circulation is minimal. At a velocity equal to ∼4 cm/s, a transition to the heterogeneous regime is

* To whom correspondence should be addressed.

† Nomenclature for this paper may be found in part 1 of the series.

S0888-5885(95)00366-6 CCC: $12.00

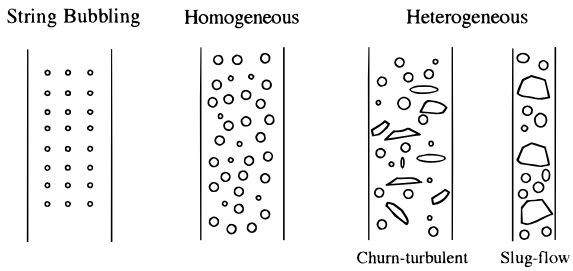

Figure 1. Flow regimes in bubble columns.

observed where the processes of bubble coalescence and breakup significantly alter the size distribution as well as other hydrodynamic properties such as axial mixing. The heterogeneous regime is characterized by severe turbulence, short circuiting of the gas by liquid circulation (channeling), and bimodal bubble size distributions. For small column diameters, the flow may begin to "slug" up the column, as shown in the figure.

On the basis of the qualitative descriptions of these flow regimes, one can conclude that heterogeneous flow is not desirable in solvent sublation, as bimodal-bubble size distributions and liquid-phase circulation adversely affect the interfacial mechanism of sublation. Additionally, operational difficulties associated with solvent−water interface control become significant due to the intense turbulence. Though many industrial columns operate in the churn-turbulent regime to maximize column throughput, the advantage of sublation is lost in this regime. One can argue then that the optimum flow regime for solvent sublation is the homogeneous regime which balances column throughput with a stable, uniform bubble size distribution. In fact, it turns out that the interfacial area is actually higher in the homogeneous regime than in the string bubbling flow regime. To understand why this is the case requires some knowledge of column hydrodynamic properties and the ability to predict them.

Over the last 35 years, there have been a vast number of bubble column studies which have investigated ways to predict hydrodynamic properties from observable quantities. Two excellent review papers (Shah *et al.*, 1982; Deckwer and Schumpe, 1993) summarize many of the correlations available for design and scaleup. In Table 1, some well-accepted correlations for gas holdup, bubble size, interfacial area, and the liquid-dispersion coefficient are listed. Of these hydrodynamic properties, the interfacial area is the most important in solvent sublation. As illustrated in the table, Akita and Yoshida (1974) showed that, for a given system, the interfacial area may be predicted solely from the gas holdup. However, in general, interfacial area is defined as $a_v = 6\epsilon/d_s$. Using the correlations for gas holdup and bubble size in Table 1, one can show how the interfacial area depends upon the gas velocity.

As can be seen from the first gas holdup correlation (Akita and Yoshida, 1973), the dependence on velocity is approximately linear at low gas velocity (homogeneous regime), but as the velocity increases, the dependence becomes less so. This is best illustrated by the second correlation for holdup (Hikita *et al.*, 1980), which shows a square-root dependence in the heterogeneous regime. In the homogeneous regime, bubble size has an approximate $^1/_2$ root dependence on velocity. However, at higher gas velocities, the bubble size has a weak inverse dependence on velocity. The reason for this is that, in the heterogeneous regime, bubble breakup and coalescence begin to dominate over bubble formation dynamics (Geary and Rice, 1991). When the effects of velocity on gas holdup and bubble size are combined, the net effect is that the *interfacial area per unit volume* of dispersion increases with approximately the square root of velocity, despite the fact that the *specific interfacial area per bubble* decreases. Since this dependence is only valid in the homogeneous regime, the implication is that, for solvent sublation, the appropriate

Table 1. Correlations for Predicting Hydrodynamic Properties in Bubble Columns

correlation	reference
Gas Holdup, ϵ	
$\frac{\epsilon}{(1-\epsilon)^4} = 0.2\left(\frac{D_c^2\varrho_l g}{\sigma}\right)^{1/8}\left(\frac{gD_c^3\varrho_l^2}{\mu_l^2}\right)^{1/12}\frac{u_g}{\sqrt{gD_c}}$	Akita and Yoshida, 1973
$u_g < 0.4$ m/s	
$\epsilon = 0.672\left(\frac{u_g\mu_l}{\sigma}\right)^{0.578}\left(\frac{\mu_l^4 g}{\varrho_l\sigma^3}\right)^{-0.131}\left(\frac{\varrho_g}{\varrho_l}\right)^{0.062}\left(\frac{\mu_g}{\mu_l}\right)^{0.107}$	Hikita *et al.*, 1980
$0.042 < u_g < 0.38$ m/s	
Bubble Size, d_s	
$\frac{\pi d_s^3}{6} \propto u_g^{1.2}$ homogeneous flow	Clift *et al.*, 1978
$d_s \propto u_g^{0.5}$ homogeneous flow	Geary and Rice, 1991
$\frac{d_s}{D_c} = 26\left(\frac{D_c^2 g\varrho_l}{\sigma}\right)^{-0.5}\left(\frac{gD_c^3\varrho_l^2}{\mu_l^2}\right)^{-0.12}\left(\frac{u_g}{\sqrt{gD_c}}\right)^{-0.12}$ heterogeneous flow	Akita and Yoshida, 1974
Interfacial Area, a_v	
$a_v D_c = \frac{1}{3}\left(\frac{D_c^2 g\varrho_l}{\sigma}\right)^{0.5}\left(\frac{gD_c^3\varrho_l^2}{\mu_l^2}\right)^{0.1}\epsilon^{1.13}$	Akita and Yoshida, 1974
Axial Dispersion Coefficient, D	
$D = 0.35 D_c^{4/3}(u_g g)^{1/3}$	Baird and Rice, 1975
$\frac{D}{u_g} \propto \lambda^n \begin{cases} \lambda \sim d_s & \text{for truly vertical columns in the homogeneous regime} \\ \lambda \sim L_c & \text{for nonvertical columns} \end{cases}$	Kantak *et al.*, 1994

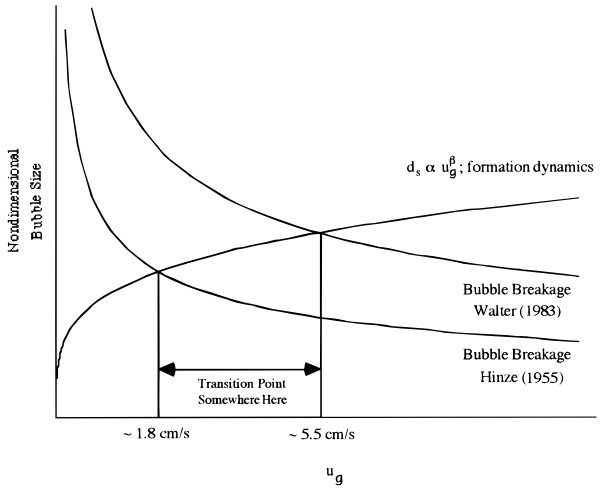

Figure 2. Bubble size as predicted by formation dynamics and breakage due to turbulence.

velocity which maximizes capacity is the upper limit of the homogeneous regime. The question is, however, what exactly is the upper limit of the homogeneous regime?

Geary and Rice (1991) showed that, as gas velocity increases, a transition occurs in which the dynamics governing bubble formation no longer control. At the transition, the process of bubble breakage determines the upper limit of the bubble size. Using their description of bubble dynamics, one can estimate bounds for the transition from homogeneous flow to heterogeneous flow. Figure 2 is a similar figure to the one presented by Geary and Rice. In the figure, two curves for bubble size, as predicted by breakage, are given. Though only one breakage curve is unique for a given system, these two curves serve as practical lower and upper bounds. The curve based on the power model represents a bubble formation model. The points of intersection shown in the figure define the most probable range of gas velocities where the transition point may be found. As stated earlier, the upper limit for the homogeneous regime is generally accepted as ≈4 cm/s, which falls in the range.

It is emphasized that the transition point is approximate and is dependent upon operating conditions (i.e., surfactant, type of liquid, etc.) and sparger design. Hills (1974) showed that the effect of pore diameter on perforated plates can affect the transition. With small pore diameters (0.4 mm), homogeneous flow was sustainable to 3 cm/s gas velocity, while for large pore diameters (1.6 mm), homogeneous flow was never observed. Flexible spargers (Rice *et al.*, 1981), whose pores expand with gas flow, have shown that the circulatory patterns can be damped, which delays the point of transition into the heterogeneous regime. Thus, it is not exactly clear what the upper limit is; however, it is clear that small improvements in sparger design have the potential to delay the transition to the heterogeneous regime. An improvement as small as 1 cm/s represents roughly a 25% increase in column capacity for those applications requiring homogeneous flow.

(b) Bubble Generation in a Shear Field. One way to extend the homogeneous flow regime to higher gas velocities is to consider other means of bubble generation which are capable of producing higher interfacial area than normally observed in bubble columns. Producing bubbles in the presence of a velocity or shear field is one example. In the field of bubble formation dynamics, a commonly used approach to predict bubble size is the "one-step" theory for constant gas flow systems (Clift *et al.*, 1978). In this approach it is assumed that the growth of a bubble occurs smoothly and only detaches when the sum of the buoyancy force and the force of gas momentum equals the sum of the retarding forces. With the presence of the velocity field, the force balance is modified to accommodate the shear force acting on the bubble. The idea is that the additional force overwhelms the surface tension such that a smaller bubble may be produced. A device using such a field is referred to here as a shear sparger.

Very little information (Johnson *et al.*, 1982; Johnson and Gershey, 1990; Marshall *et al.*, 1993) is available on the subject of shear spargers, and no studies as to their application in bubble columns have been reported. Johnson *et al.* (1982) reported using a shear field set up between two parallel plates (one being a porous frit and the other a solid disk) to produce small bubbles for marine applications. Their experiments were conducted on a very small scale (air flow rate ~10 cm^3/min). All bubble radii measured in their studies were generally around 30 μm, with no bubbles greater than 200 μm. Unlike most investigators who measure bubbles in the bulk phase, these investigators measured the bubbles as they exited the sparger. For small-scale systems, such as theirs, the bubble sizes that they measured are most likely representative of the bulk distribution. For large-scale bubble columns, where coalescence and turbulent mixing occur, bubbles measured at the sparger are not representative of the bulk distribution; however, the data do represent the lower practical limit for bubble size obtainable in bubble columns. The same authors also investigated the effect of a shear field set up in an annulus (Johnson and Gershey, 1990). Results from that study showed mean bubble sizes around 75 μm. Because of the simplicity of construction and operation of that sparger, a similar sparger, referred to here as an annular shear sparger, has been included in this study.

Experimental Section

(a) Apparatus. Two different bubble columns were used for hydrodynamic studies. The first column, shown in Figure 3, was part of a three-phase, continuous sublation process. It consisted of a Pyrex glass column with an inside diameter of 4 in. (0.1016 m) and a length of 5 ft (1.524 m). The column was mounted on a square plate of Lexan (polycarbonate), which was supported by four metal legs. The legs were attached to a large stainless-steel spill pan (not shown in the figure) and were adjustable so that the column could be aligned near-perpendicular with the horizontal plane. Mounted on the top of the column was a cylindrical overflow reservoir made of Lexan, which had an inside diameter of 11 in. (0.2794 m) and a height of 10.5 in. (0.2667 m). The reservoir was seated approximately 4 in. from the top of the column and was sealed with an O-ring and a thin coating of Dow Corning silicone grease. The function of the overflow reservoir was to prevent the solvent from being entrained and mixed throughout the column. As shown in the figure, the process was equipped with the necessary ancillary equipment to accommodate continuous countercurrent operation. The water and solvent flow rates were controlled by FMI metering pumps, and the air flow rate was controlled

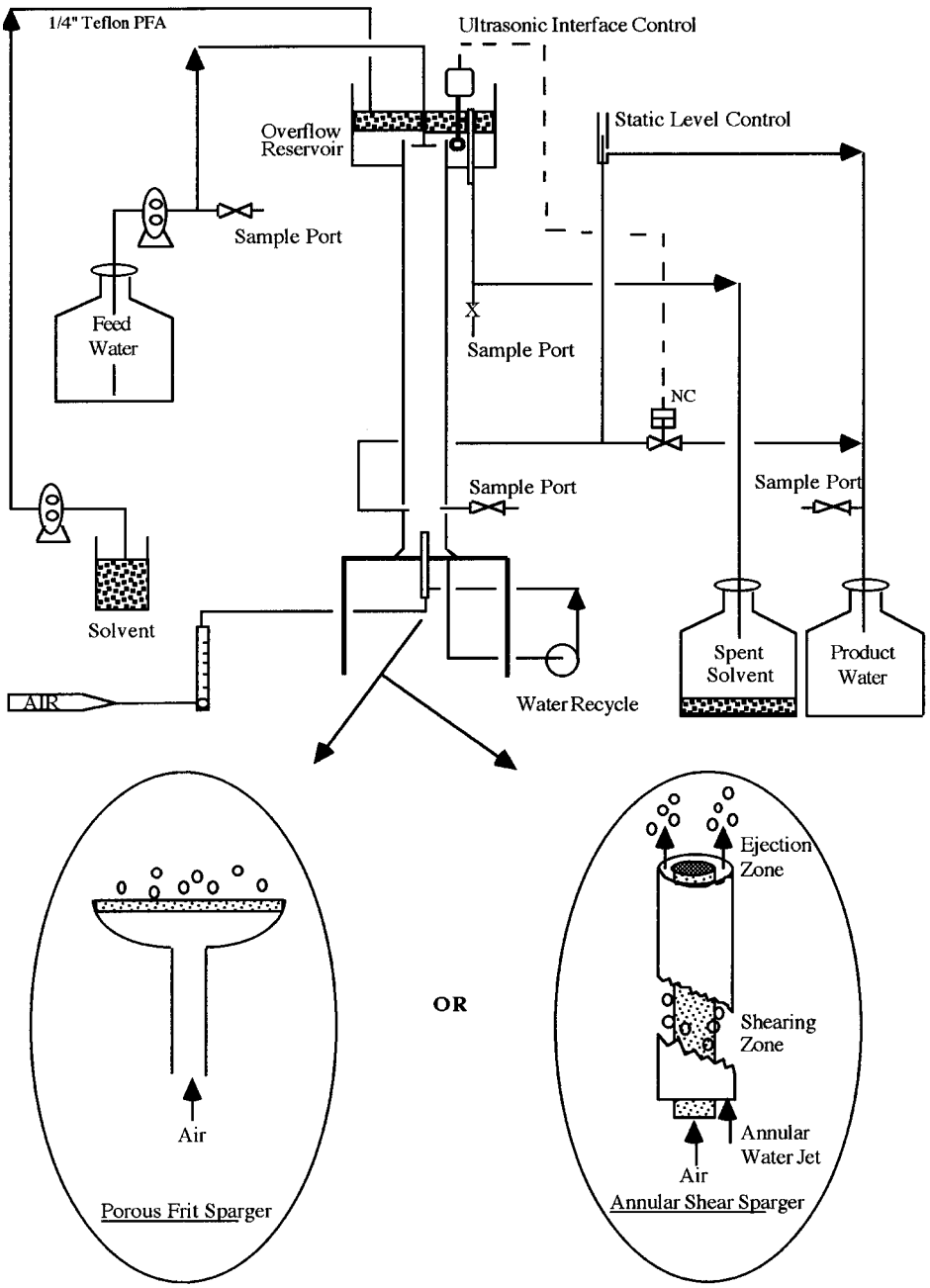

Figure 3. Schematic of pilot sublation process (4 in. diameter column).

by an Omega flow tube. The range of possible flow rates were: 0−139 mL/min for water, 0−19 mL/min for solvent, and 0−17340 mL STP/min for air. A $^1/_4$ in. U-tube (static control) was used to control the level in the column, while an Omega ultrasonic interface switch (Model LV-241) and a solenoid valve were used to control the position of the solvent−water interface.

Two types of gas spargers were used in the column and appear at the bottom of Figure 3. The first was a fine porous glass frit having a diameter of 0.09 m and an estimated mean pore size of 1.7×10^{-6} m. The second gas sparger was an annular shear sparger obtained from the Mott Metallurgical Corp., who commercially manufactures these devices. The porous element used in this particular sparger was a cylinder made of 316SS having an area of 0.1 ft^2 (92.9 cm^2) and mean pore size of 2.0×10^{-6} m. The element was placed in a $^3/_4$ in. NPT-PVC pipe, and an external pump loop was used to set up a velocity field (water jet) in the annulus.

The second bubble column used for hydrodynamic studies was made of Plexiglass and appears in Figure 4. The dimensions of the column were 5.5 in. (0.1397 m) i.d. by 7 ft (2.134 m) tall. As shown in the figure, a series of pressure taps equally spaced up the column were available for differential pressure measurements. The overflow reservoir at the top of the column was 18 in. (0.4572 m) i.d. by 18 in. (0.4572 m) tall. The column mount was secured to the floor by a ball-bearing pivot, which was used to align the column *perfectly vertical* (Rice and Littlefield, 1987). Two gas spargers were also used in this column. The first was a perforated latex membrane (Flexisparger) whose dimensions and other characteristics have been described elsewhere (Geary, 1992). The second was an annular shear sparger similar to the one used in the smaller column; however, the porous surface area was 0.05 ft^2 (46.45 cm^2).

(b) Gas Holdup Measurements. In the small column, gas holdup was determined by measuring the change in liquid height, Δx, with and without air flow.

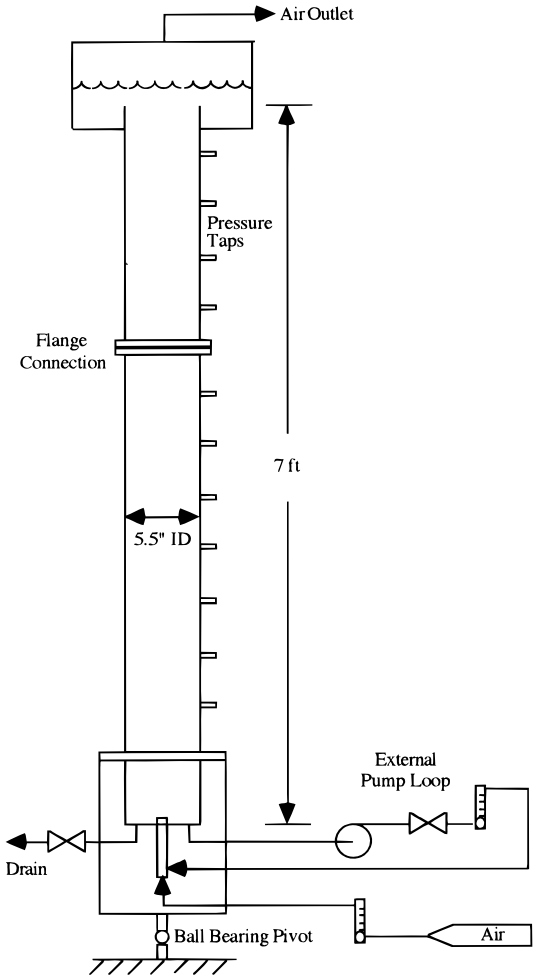

Figure 4. Schematic of pilot sublation process (5.5 in. diameter column).

The traditional equation used to calculate gas holdup was modified to accommodate the difference in diameter between the column and the overflow reservoir,

$$\epsilon = \frac{\Delta x\left(\frac{11\text{ in.}}{4\text{ in.}}\right)^2}{\Delta x\left(\frac{11\text{ in.}}{4\text{ in.}}\right)^2 + L_o} \tag{1}$$

where L_o is the height of water without air flow. Gas holdup experiments without the overflow reservoir were conducted which showed that eq 1 predicted the same value as the unmodified equation. In the large column, gas holdup was determined by measuring the differential pressure across the height of the column with a manometer. The gas holdup was calculated as

$$\epsilon = \left(\frac{\varrho_m - \varrho_l}{\varrho_l}\right)\frac{\Delta h_m}{\Delta h_{col}} \tag{2}$$

where ρ_m is the density of the manometer fluid (miriam red) and ρ_l is the density of pure water. The measurements, Δh_m and Δh_{col}, are the differential height change of miriam red in the manometer and the height between the bottommost and uppermost pressure taps on the column, respectively. To derive eq 2, the pressure drop associated with the lines between the pressure taps and the manometer must be accounted for, as the density in these lines is not the same as that in the bubble column. Equation 2 is only valid when the manometer is positioned between the pressure taps.

(c) Bubble Size Measurements. Bubble size measurements in the small column were determined using a photographic technique using a 35 mm camera positioned 1.5 ft from the column and 2 ft above the sparger. A sheet of white paper was placed behind the column to provide a uniform background, and a 100-W incandescent lamp fixed 90° relative to the field of view was used as the primary light source (the room's fluorescent lights provided secondary lighting). The camera was focused upon a 38 × 38 mm cross section centered approximately in the middle of the column. A template (graph paper) was placed on the exterior of the column in the field of view which served as a scale for image analysis. The shutter speed of the camera was set at 0.001/s. The film used was 400 ASA, but the photographs were taken as 3200 ASA and were underexposed and overdeveloped. This procedure produced the best results for distinguishing the air bubbles from the water. The photographs were enlarged to 8 in. × 10 in. prints and still-imaged; video (super-VHS) of the enlarged prints was collected and recorded to computer disks. The imaging software which was used to record and analyze the data was JAVA, a product from Jandel Scientific Corp. In most cases, approximately 200 bubble size measurements were taken for each experimental condition and were used to calculate the sauter mean bubble diameter,

$$d_s = 2a = \frac{\sum_i n_i d_i^3}{\sum_i n_i d_i^2} \tag{3}$$

(d) Dispersion Measurements. Liquid dispersion coefficients in the small column were determined at different air flow rates by injecting a tracer (dye) into the top of the column and measuring the time for the tracer front to traverse a fixed distance, x. For each experiment, two times were recorded, one at $x_1 = 27$ in. and one at $x_2 = 54$ in. Equation 4 was used to convert these measurements into dispersion coefficients. The derivation (Cussler, 1987) of eq 4 involves equating the solution for the diffusion equation with the Gaussian function to obtain $D = \sigma^2/2t$, where σ^2 is the variance. Next, $x^2/2$, which is a good approximation for the variance, is substituted for σ^2.

$$D = x^2/4t \tag{4}$$

The materials used in the hydrodynamic experiments were distilled water, light white mineral oil supplied by Sigma−Aldrich, and instrument air supplied by LSU plant utilities.

Results and Discussion

(a) Gas Holdup. Figure 5 shows the dependence of gas holdup upon superficial air velocity, u_g. As points of reference, well-accepted correlations for gas holdup (Akita and Yoshida, 1973; Hikita *et al.*, 1980) have been included in the figure. Recently (Deckwer and Schumpe, 1993), it has been reported that these correlations provide good, conservative estimates of the gas holdup in bubble columns; however, the authors stressed that such correlations do not apply to the limited number of applications involving the bubbly flow regime. Gener-

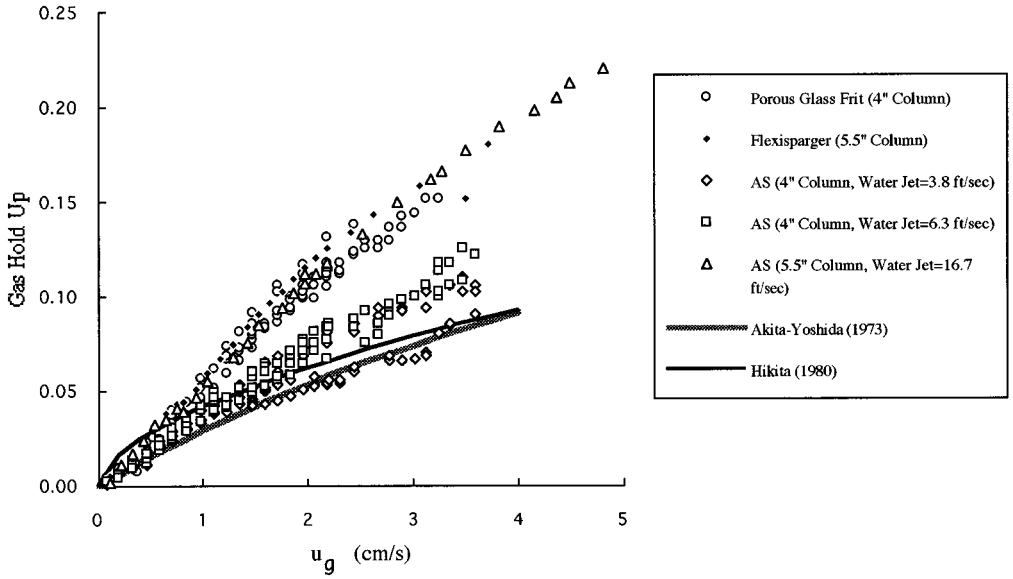

Figure 5. Gas holdup versus superficial gas velocity.

ally, gas holdup data conform to power-law models of the type $\epsilon = \alpha u_g^{\beta}$. For the porous glass frit and the flexible rubber sparger, β was calculated as 1.14 (α = 0.049) for the entire range of velocities studied. This near-linear dependence is characteristic of the homogeneous regime and is not surprising for these spargers. Moreover, it was not surprising that there was no observable effect of column diameter on gas holdup since gas holdup is generally independent of column diameter for diameters greater than 10 cm (Shah *et al.*, 1982).

The results of the gas holdup measurements collected from the annular shear sparger are also shown in Figure 5. Measurements were recorded for three different water jet velocities, 3.8 (1.15), 6.3 (1.92), and 16.7 ft/s (5.09 m/s). The low-velocity data were collected from the 4 in. diameter column as the water jet in this column was limited to 6.3 ft/s. As can be seen from the figure, increasing the water jet velocity, or equivalently the shear force over the porous surface, improved the gas holdup in the column. Attempts were made to operate at higher gas holdups by further increasing the jet velocity, however, the holdup data collected at 16.7 ft/s was observed to be the upper limit. For general aeration applications, the manufacturer recommends a minimum velocity of 10 ft/s. Interestingly, the data conform almost exactly (β = 1.03 and α = 0.049) with that collected from the porous frit and the flexible rubber sparger. This would indicate that the maximum value of gas holdup for air−water (without the use of surfactant, solvent, or salts) has been reached.

The most important observation about the data for the shear sparger is that homogeneous flow is maintained up to 5 cm/s as indicated in the figure, whereas homogeneous flow was only sustainable up to 4 cm/s for the flexible rubber sparger.

(b) Bubble Size. Bubble size measurements were collected for the porous frit and the 0.1 ft^2 annular shear sparger (jet velocity = 6.3 ft/s). These measurements were compiled into 12 histograms which show the relative size and distribution dependencies upon superficial gas flow rate. The histograms are presented in the Appendix as Figure 11. In the case of the frit sparger, the general trend observed in the histograms was that, as the gas flow rate increased, the bubble size and the breadth of the size distribution increased. Again, this behavior is a classic example of the homogeneous flow regime. However, in the case of the annular shear sparger, this general trend was not observed.

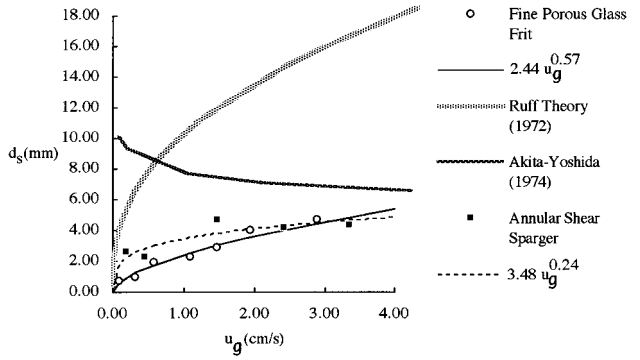

Figure 6. Sauter mean bubble size versus superficial gas velocity.

First, the bubble size dependence on gas flow rate for the shear sparger was much weaker than it was for the frit sparger. This observation is illustrated in Figure 6 where the sauter mean diameter is plotted versus superficial gas velocity. As one can see, the data obtained from the frit sparger fit well to a square-root function, whereas the data taken from the annular shear sparger showed a weaker dependence on velocity, 0.24. This dependence on velocity was sufficiently weak that, at velocities greater than 1.0 cm/s, the sauter mean diameter became effectively constant at about 4.5 mm. Also shown in Figure 6 are two correlations for bubble size. The first is a semiempirical correlation developed by Ruff (Clift *et al.*, 1978) which applies to bubble formation at a single orifice and is used as a point of reference. The second correlation, that of Akita and Yoshida (1974), is listed in Table 1. It has a velocity dependence which resembles that of a breakage curve.

The second observation drawn from the histograms was that the breadth of the size distribution for the annular shear sparger was independent of gas flow rate. This behavior was not anticipated; however, it was a direct consequence of the first observation. The reason is clear when one examines the expression for the sauter mean diameter eq 3. It is nothing more than a statistical moment of the data. For the sauter mean diameter to show such a weak dependence upon velocity, the distribution of diameters must be similar for each

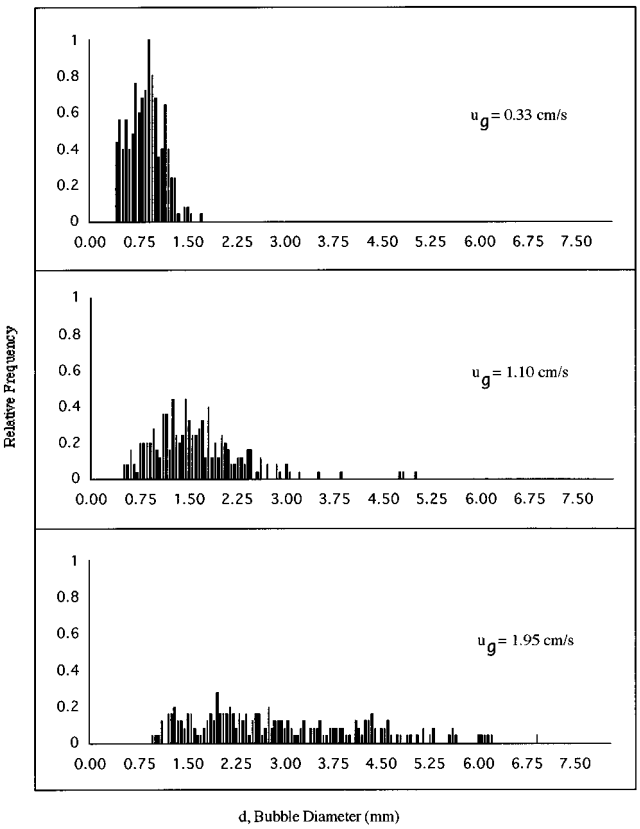

Figure 7. Relative frequency plots for the bubbles generated from the porous, glass frit (4 in. diameter column).

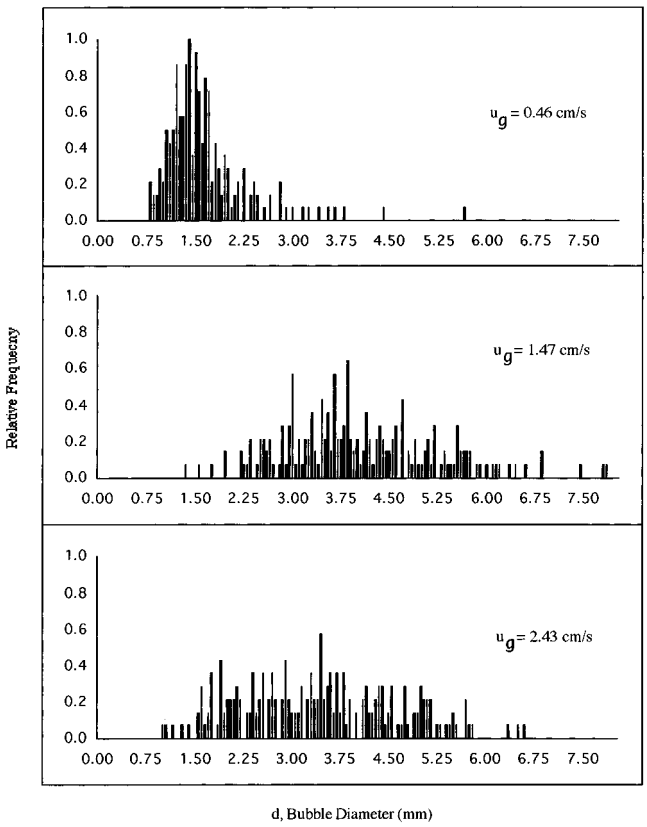

Figure 8. Relative frequency plots for the bubbles generated from the annular shear sparger (4 in. diameter column).

velocity. To illustrate this, normalized histograms for each sparger are compared in Figures 7 and 8. One can see in the figures that, while the bubble size and distribution increase with velocity for the frit sparger, a near uniform distribution develops for the shear sparger.

One explanation why the annular shear sparger produced bubbles seemingly independent of gas velocity was based upon visual observations of the ejection zone which is located just above the shear sparger (see Figure 3). For gas velocities greater than 1 cm/s, a plume of fine bubbles and water developed, which extended approximately 8 cm into the column. The appearance of the plume was milky-white and resembled nucleation bubbles resulting from degassing pressurized water. At gas velocities less than 1.0 cm/s, the plume was no longer milky. There was a clear distinction between air bubbles and the streamlines of the water jet. It is known that a local CSTR region develops above gas spargers in bubble columns (Rice *et al.*, 1990). In the case of the shear sparger, the rate of local circulatory motion in this region was intensified greatly due to the water jet. A few centimeters above the plume, there was a sharp gradient in bubble size. Whereas the bubbles in the plume were estimated to be on the order of 100 μm, the bubbles above the plume were on the order of 4 mm. It was clear that most of the coalescence in the column occurred in this CSTR region. The bubbles leaving this region rose up the column uniformly distributed across the column diameter and experienced very little breakage or coalescence. In effect, the circulatory motion set up by the water jet tended to buffer the breakage and coalescence. It was speculated that this buffering effect may be the reason why the bubble size seems to be independent of gas velocity in the homogeneous flow regime.

Alternatively, it may be argued that the bubble size distribution is dictated by bubble formation dynamics which occur at the orifice or pore. For conventional gas spargers (i.e., porous frit) operating at low gas flow rates, a single bubble forms above an orifice when the gas momentum through the orifice exceeds the surface tension. As the gas flow rate is increased through the orifice, the rate of bubble formation becomes so rapid that, after one bubble detaches, another forms beneath it and the two coalesce into a "double bubble" (LaNauze and Harris, 1974; Payne and Prince, 1975; Marmur and Rubin, 1976; Wilkinson and Dierendonck, 1994). Consequently, the shape and size of the orifice affect the shift from single bubbling to double bubbling. The extent of double bubbling influences bulk properties, such as breakage and coalescence, the two properties which determine the flow regime. In the case of the rubber membrane, as the gas flow rate is increased, the rubber sheet inflates and expands. Thus, the orifice diameters increase, reducing the gas momentum. This effect delays the shift from single bubbling to double bubbling and ultimately delays the transition to the heterogeneous regime. In the case of the shear sparger, liquid momentum set up parallel to the sparger surface is utilized to shear bubbles off the surface before they coalesce into double bubbles. This process is unique in that it is independent of gas momentum. The effect of the shear sparger is to delay the transition to the heterogeneous regime in two ways. First, in a fashion similar to that of the rubber membrane, the shift from single bubbling to double bubbling is delayed. In fact, based upon the observed bubble sizes in the ejection zone, double bubbling is essentially eliminated. Second, the absence of double bubbling allows for a more uniform bubble size distribution which tends to maintain the equilbrium between breakage and coalescence

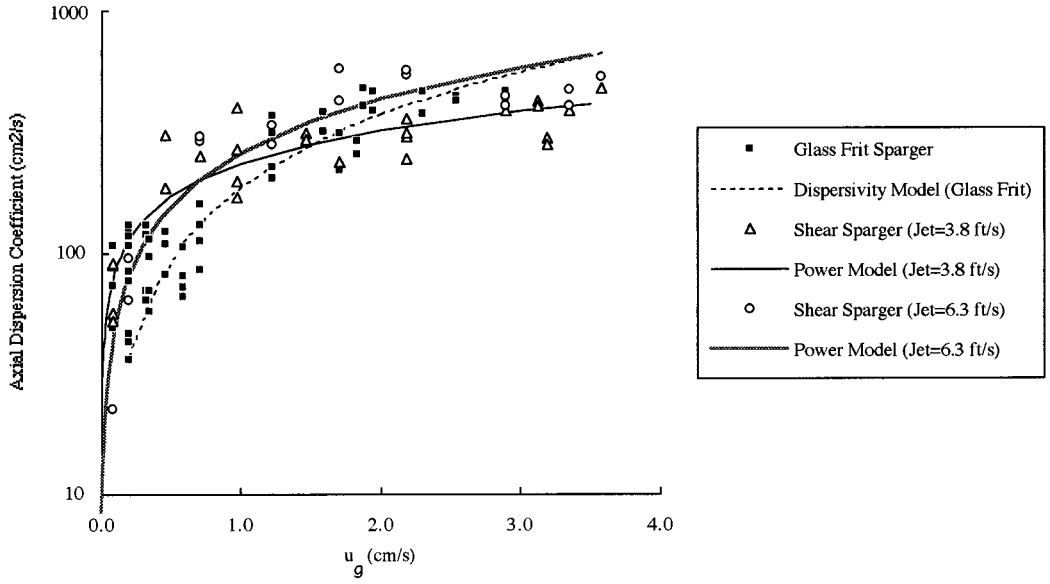

Figure 9. Axial dispersion coefficient versus superficial gas velocity.

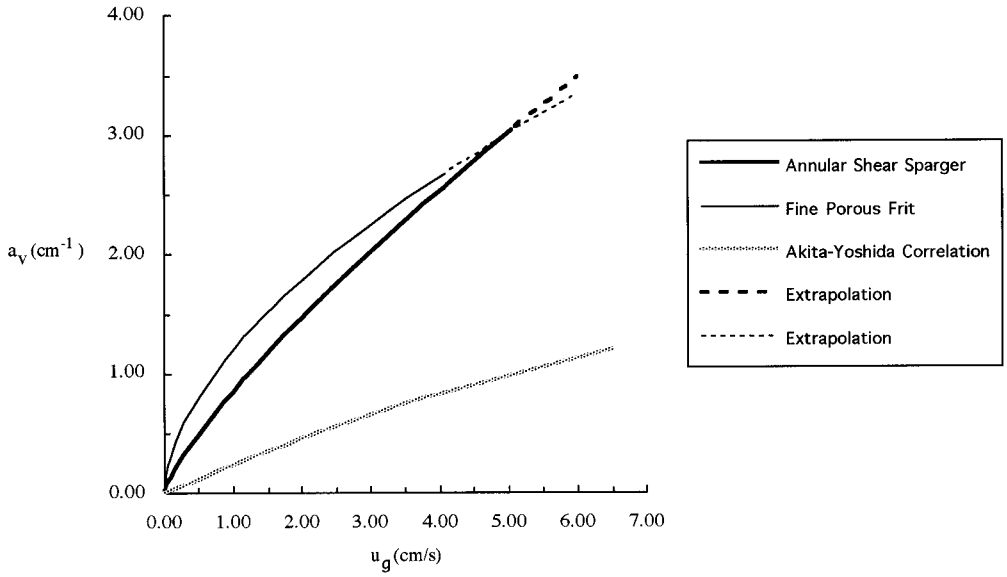

Figure 10. Predicted interfacial area per unit volume versus superficial gas velocity.

at higher superficial gas velocities. Eventually, however, an imbalance between these two processes occurs and the flow becomes heterogeneous.

(c) Axial Dispersion Coefficient. Dispersion measurements were obtained for the 4 in. column. There was no significant difference between the porous frit and the 0.1 ft^2 shear sparger as shown in Figure 9; however, one may argue that small biases exist. Therefore, each data set appearing in the figure has been fit with its own power law to illustrate the small biases. Overall, the entire data set conforms to a power-law model with a 0.62 dependence on velocity. This dependence falls between bubbly flow (linear dependence) and churn-turbulent (one-third dependence) (Rice *et al.*, 1981). At velocities greater than 1.0 cm/s, the dispersion in the column is effectively a constant equal to approximately 375 cm^2/s, which is not too surprising given the low L/D_c of 15 for the 4 in. column. Deckwer *et al.* (1974), using a better technique for dispersion measurement, has reported values in the range of 275−300 cm^2/s for the same range of velocities studied here, but for columns with L/D_c ratios around 30.

Recently (Kantak *et al.*, 1994), it has been shown that the same approach used to describe dispersion in porous media applies well to bubble columns. The approach involves identifying the correct length scale, λ, governing the column dynamics and relating it to the dispersivity, α_L, which is defined as the ratio of the measured axial dispersion coefficient to the gas velocity as indicated in the bottom of Table 1. The authors pointed out that there was no restriction on using the in-situ velocity rather than the superficial velocity; however, for the heterogeneous flow regime, they found that the in-situ velocity worked better. The equations for dispersivity are

$$\alpha_L \equiv D/u_g = f(\lambda) \tag{5a}$$

$$\alpha_L \equiv D/(u_g/\epsilon) = h(\lambda) \tag{5b}$$

For truly vertical columns operating in the homogeneous regime, λ is proportional to the bubble size. In the heterogeneous regime, λ then approaches the column diameter. For nonvertical columns operating either in the homogeneous or heterogeneous regime,

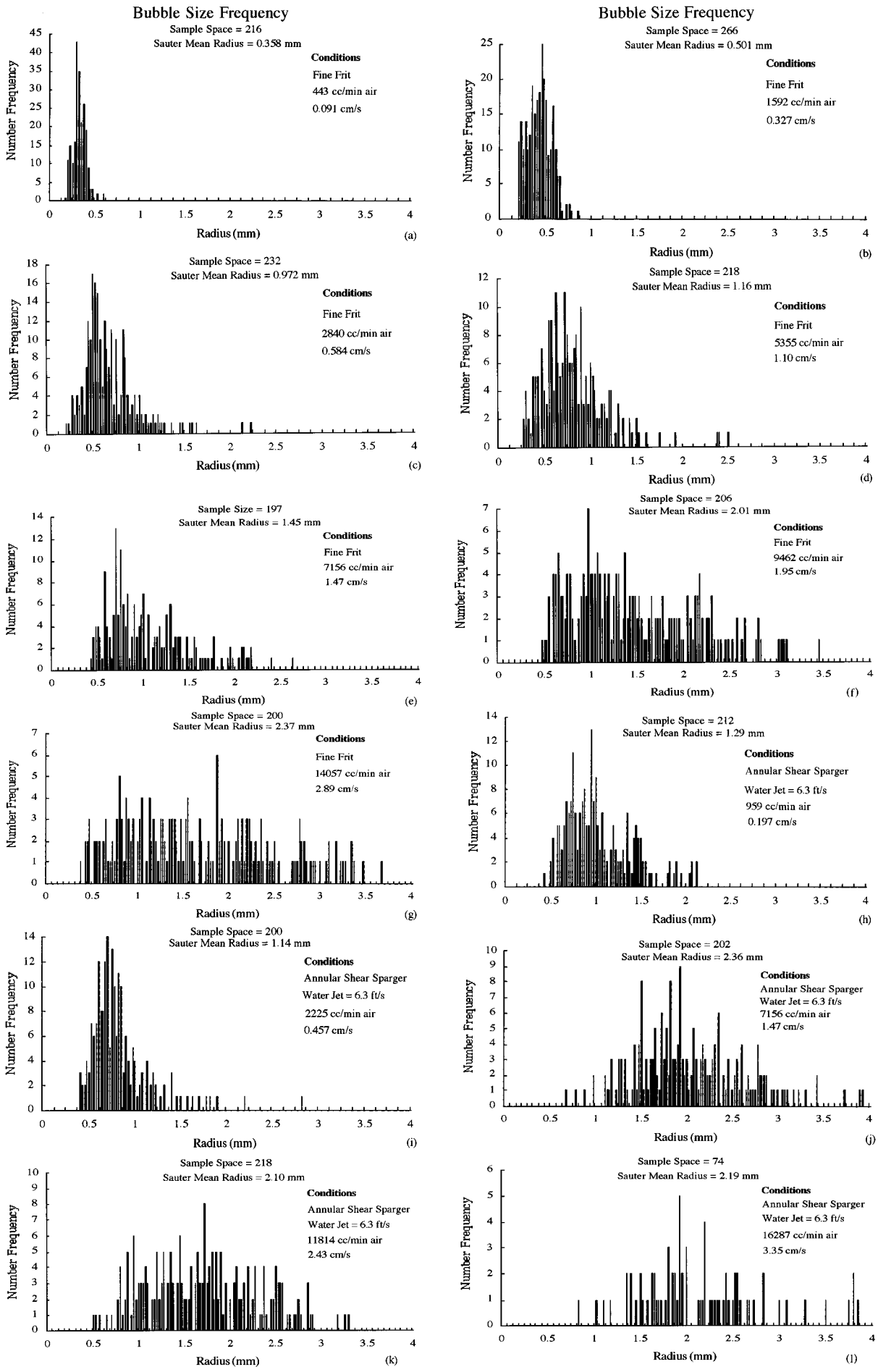

Figure 11. Bubble size histograms.

such as the 4 in. column studied here which was only near vertical, λ approaches the length scale of the column height (Rice and Littlefield, 1987). As shown in Figure 9, the dispersivity model was used to fit the porous frit data; eq 5a was used. From a regression analysis of the data, $f(\lambda)$ was found to be 187.2 cm, indicating a linear relationship. The error associated with this fit was ±10%. This length was compared to an effective column height (adjusted for the overflow reservoir) of about 165 cm. This agreement was consistent with the length-scale arguments.

Though not shown in the figure, it was calculated from eq 5b that the average dispersivity for the annular shear sparger was $h(\lambda) = 11$ cm with a standard deviation of 3 cm. What is interesting about this result is that it suggested the appropriate length scale for the shear sparger was the column diameter (4 in. = 10.16 cm) despite the fact that the column was not truly vertical. The reason for this is not clear; however, it is most likely related to the buffering effect described above.

Effect on Interfacial Area. The dependence of interfacial area on gas velocity was determined by combining the power-law models developed here for gas holdup and bubble size. In Figure 10, the interfacial areas for the porous frit and shear sparger are compared to the correlation for the interfacial area listed in Table 1. The solid part of the curves in the figure apply to the homogeneous regime, and the broken lines indicate extrapolation. As one can see, the Akita−Yoshida (1974) correlation predicts very conservative values. The data obtained from the two spargers are much more realistic, as most interfacial area data collected from bubble columns range between 2 and 4 cm^{-1} (Shah *et al.*, 1982). The curve for the frit sparger has a functionality similar to that of those curves presented in the same paper for perforated and sintered plates. The near-linear dependence for the shear sparger stems from the fact that the bubble size for this sparger has a weaker dependence on gas velocity. The important observation is that the shear sparger delays the transition to the heterogeneous regime by about 1 cm/s. This makes it possible to operate at a higher interfacial area per unit volume such as 3 cm^{-1}, a value more common to the heterogeneous regime.

Conclusion

It was concluded that solvent sublation is not limited to the string bubbling flow regime (<0.2 cm/s gas velocity) as generally believed by previous investigators. In fact, it was shown that, by including the effects of gas holdup on the interfacial area, the benefit of solvent sublation is best realized at the upper limit of the homogeneous regime. Therefore, past arguments which stated that the scalability of solvent sublation is limited are not accurate.

Hydrodynamic data were collected from three types of gas spargers: a fine porous, glass frit, a flexible rubber membrane (Flexisparger), and an annular shear sparger. Gas holdup results indicated that the shear sparger altered the column dynamic properties such that the transition from the homogeneous to the heterogeneous flow regime was delayed. The transition for the porous frit was approximately at 2.5−3.0 cm/s, while that of the rubber membrane was 4.0 cm/s. The transition to the heterogeneous regime for the shear sparger was approximately 5.0 cm/s, a 25% improvement over the rubber membrane.

Results from bubble size measurements indicated that, for the shear sparger, the dependence of bubble diameter on gas velocity was approximately $^1/_4$. This compared to a square-root dependence for the porous frit, which is the same dependence predicted by formation theories and correlations. The weaker dependence was attributed to the intensified circulation in the small CSTR region located above the shear sparger. This region tended to buffer the processes of coalescence and breakage in the column. It was observed that the bubbles ejected from the shear sparger were much smaller (~100 μm) than the bubbles in the bulk (~4 mm). The sharp gradient in size occurred in the local CSTR region.

Axial dispersion measurements indicated that there were no appreciable differences in the extent of mixing between the porous frit and the shear sparger. However, calculations of the length scales associated with these spargers were different. As expected, due to the fact that the column was not truly vertical, the length scale for the porous frit was on the order of the column height. The length scale of the shear sparger, though, was on the order of the column diameter. Though it was not clear, the difference in the length scale was attributed to the reduced coalescence and breakage associated with the shear sparger.

Finally, the results of the gas holdup and bubble size measurements were used to predict the interfacial area generated by the frit and shear spargers. In the case of the shear sparger, an interfacial area per unit volume of 3 cm^{-1} was possible at a gas velocity of 5 cm/s, which for this sparger is in the homogeneous flow regime. This interfacial area rivaled those areas often observed in the heterogeneous flow regime.

As further developments are made in the field of sparger design, it is foreseeable that the homogeneous regime may be further extended to higher gas velocities. Thus, one may conclude that solvent sublation and other related low-pressure adsorptive processes may soon become viable options for industry. These aspects will be explored in part 3 of this series with actual data on the removal of several hydrophobic organics from wastewaters.

Acknowledgment

This work was supported in part by the National Science Foundation/EPSCOR program {NSF/LaSER (1992−96) ADP-03}.

Appendix

Parts a−g of Figure 11 are bubble size histograms for the fine porous, glass frit operating in the 4 in. diameter column. Parts h−l are bubble size histograms for the 0.1 ft^2 annular shear sparger operating in the 4 in. diameter column.

Literature Cited

Akita, K.; Yoshida, F. Gas Holdup and Volumetric Mass Transfer Coefficient in Bubble Columns. *Ind. Eng. Chem. Process Des. Dev.* **1973**, *12*, 76.

Akita, K.; Yoshida, F. Bubble Size, Interfacial Area, and Liquid Phase Mass Transfer Coefficients in Bubble Columns. *Ind. Eng. Chem. Process Des. Dev.* **1974**, *13*, 84.

Baird, M. H. I.; Rice, R. G. Axial Dispersion in Large Unbaffled Columns. *J. Chem. Eng.* **1975**, *9*, 171−174.

Clift, R.; Grace, J. R.; Weber, M. E. Formation and Breakup of Fluid Particles. *Bubbles, Drops, and Particles*; Academic Press: San Diego, 1978; pp 321−328.

Cussler, E. L. Dispersion. *Diffusion: Mass Transfer in Fluid Systems*; Cambridge University Press: Cambridge, U.K., 1987; Chapter 4.

Deckwer, W. D.; Schumpe, A. Improved Tools for Bubble Column Reactor Design and Scale-Up. *Chem. Eng. Sci.* **1993**, *48* (5), 889−911.

Deckwer, W. D.; Burckhart, R.; Zoll, G. Mixing and Mass Transfer in Tall Bubble Columns. *Chem. Eng. Sci.* **1974**, *29*, 2177−2188.

Geary, N. W. On Bubble Columns. Ph.D. Dissertation, Louisiana State University, Baton Rouge, LA, 1992.

Geary, N. W.; Rice, R. G. Bubble Size Prediction for Rigid and Flexible Spargers. *AIChE J.* **1991**, *37* (2), 161−168.

Hikita, J.; Asai, K.; Tanigawa, K.; Segawa, K.; Kitao, M. Gas Holdup in Bubble Column. *J. Chem. Eng.* **1980**, *20*, 59.

Hills, J. H. Radial Non-Uniformity of Velocity and Voidage in a Bubble Column. *Trans. Inst. Chem. Eng.* **1974**, *52*, 1.

Hinze, J. O. Fundamentals of the Hydrodynamic Mechanism of Splitting in Dispersion Processes. *AIChE J.* **1955**, *1*, 289.

Ishii, M.; Zuber, N. *Thermo-Fluid Dynamic Theory of Two-Phase Flow*; OParisE: Evroller, 1975.

Johnson, B. D.; Gershey, R. M. Bubble Formation at a Cylindrical Frit Surface in a Shear Field. *Chem. Eng. Sci.* **1990**, *46*(10), 2753−2756.

Johnson, B. D.; Gershey, R. M.; Cooke, R. C.; Sutcliffe, W. H. A Theoretical Model for Bubble Formation at a Frit Surface in a Shear Field. *Sep. Sci. Technol.* **1982**, *17* (8), 1027−1039.

Kantak, M. V.; Shetty, S. A.; Kelkar, B. G. Liquid Phase Backmixing in Bubble Column Reactors—A New Correlation. *Chem. Eng. Commun.* **1994**, *127*, 23−34.

LaNauze, R. D.; Harris, I. J. Gas Bubble Formation at Elevated System Pressures. *Trans. Inst. Chem. Eng.* **1974**, *52*, 337−348.

Marmur, A.; Rubin, E. A Theoretical Model for Bubble Formation at An Orifice Submerged in an Inviscid Liquid. *Chem. Eng. Sci.* **1976**, *31*, 453−463.

Marshall, S. H.; Chudacek, M. W.; Bagster, D. F. A Model for Bubble Formation from an Orifice with Liquid Cross-Flow. *Chem. Eng. Sci.* **1993**, *48* (11), 2049−2059.

Payne, G. J.; Prince, R. G. H. The Transition from Jetting to Bubbling at a Submerged Orifice. *Trans. Inst. Chem. Eng.* **1975**, *53*, 209−223.

Rice, R. G.; Littlefield, M. A. Dispersion Coefficients for Ideal Bubbly Flow in Truly Vertical Bubble Columns. *Chem. Eng. Sci.* **1987**, *42* (8), 2045−2053.

Rice, R. G.; Tupperainen, J. M.; Hedge, R. M. Dispersion and Holdup in Bubble Columns—Comparison of Rigid and Flexible Spargers. *Can. J. Chem. Eng.* **1981**, *59* (12), 677−687.

Rice, R. G.; Barbe, D. T.; Geary, N. W. Corrleation of Nonverticality and Entrance Effects in Bubble Columns. *AIChE J.* **1990**, *36* (9), 1421−1424.

Shah, Y. T.; Kelkar, B. G.; Godbole, S. P.; Deckwer, W. D. Design Parameters Estimations for Bubble Column Reactors. *AIChE J.* **1982**, *28* (3), 353−379.

Shibata, J.; Tokunaga, J. Removal of Toxic Organic Compound from Aqueous Solution by Solvent Sublation. *Technol. Rep. Kansai Univ.* **1994**, *36*, 61−69.

Valsaraj, K. T. Removal of Organics from Water by Non-foaming Flotation. In *Flotation-Science and Engineering*; Matis, K. A., Ed.; Marcel Dekker: New York, 1995; pp 365−383.

Valsaraj, K. T.; Thibodeaux, L. J. Studies in Batch and Continuous Solvent Sublation. II. Continuous Countercurrent Solvent Sublation of Neutral and Ionic Species from Aqueous Solutions. *Sep. Sci. Technol.* **1991**, *26* (3), 367−380.

Valsaraj, K. T.; Thoma, G. J.; Thibodeaux, L. J.; Wilson, D. J. Nonfoaming Adsorptive Bubble Separation Processes. *Sep. Technol.* **1991**, *1*, 234−243.

Walter, J. W. Bubble Breakup and Mass Transfer in Gas−Liquid Contactors. Ph.D. Dissertation, University of California at Berkley, Berkley, CA, 1983.

Wilkinson, P. M.; Dierendonck, L. L. V. A Theoretical Model for the Influence of Gas Properties and Pressure on Single-Bubble Formation at an Orifice. *Chem. Eng. Sci.* **1994**, *49*, 1429−1438.

Received for review June 16, 1995
Accepted February 15, 1996[⊗]

IE950366Y

[⊗] Abstract published in *Advance ACS Abstracts*, April 1, 1996.